Talanta 201 (2019) 350–357

Contents lists available at ScienceDirect

Talanta

journal homepage: www.elsevier.com/locate/talanta

Fabrication of a novel biosensor for biosensing of bisphenol A and detection of its damage to DNA

Ali R. Jalalvand[a,*], Ali Haseli[a], Farshad Farzadfar[b], Hector C. Goicoechea[c]

[a] Research Center of Oils and Fats, Kermanshah University of Medical Sciences, Kermanshah, Iran
[b] Non-Communicable Diseases Research Center, Endocrinology and Metabolism Population Sciences Institute, Tehran University of Medical Sciences, Tehran, Iran
[c] Laboratorio de Desarrollo Analítico y Quimiometría (LADAQ), Cátedra de Química Analítica I, Universidad Nacional del Litoral, Ciudad Universitaria, CC 242, S3000ZAA, Santa Fe, Argentina

ARTICLE INFO

Keywords:
Bisphenol A
DNA damage
Biosensor

ABSTRACT

In this work, a novel electrochemical biosensor has been fabricated based on step-by-step modification of a glassy carbon electrode (GCE) with methylene blue (MB)-DNA/multiwalled carbon nanotubes (MWCNTs)-chitosan (CS)/palladium nanoparticles (Pd NPs)/fullerene C_{60} (C_{60}) for voltammetric and impedimetric detection of DNA damage induced by bisphenol A (BPA). Modifications applied to the GCE were characterized by cyclic voltammetry (CV), differential pulse voltammetry (DPV), electrochemical impedance spectroscopy (EIS) and scanning electron microscopy. The EIS and DPV responses of the biosensor were increased and decreased, respectively, by the DNA damage induced by BPA which led us to develop novel systems for detection of DNA damage. Our records confirmed that the biosensor was able to rapid and sensitive detection of DNA damage induced by BPA. Finally, according to the developed systems for detection of DNA damage, we have developed voltammetric and impedimetric methods for determination of BPA.

1. Introduction

Bisphenol A (BPA, Fig. 1) is an industrial compound which is widely used in fabrication of a variety of consumer products such as food cans, nursing bottles and beverage vessels. BPA is a hazardous material which is able to cause DNA damage even at very low concentrations [1]. Therefore, detection of DNA damage induced by of BPA and determination of BPA at trace levels are very important [2,3]. Various methods such as electrophoresis [4,5], spectroscopic methods [6], the DNA chip, molecular probe technologies [7] and electrochemical methods [8–11] have been reported for detection of DNA damage. Standard methods for BPA determination are including mass spectrometry-gas chromatography (GC-MS), liquid chromatography-mass spectrometry (LC-MS) and LC with different detections such as fluorescence, electrochemical and UV [12]. Although these methods are accurate and reliable, but they are expensive and time-consuming, and also require high technological instrumentation. Therefore, developing novel analytical methods which are able to rapid and sensitive determination of BPA are highly needed. Among the available analytical methods, electrochemical sensors and biosensors are interesting because their response is fast, sensitive, selective, stable, repeatable and reproducible.

Generally, to increase the sensitivity and selectivity of electrochemical sensors, they are assisted by chemometric methods or their platform is modified with different modifiers [13,14]. Modification of the platform of the electrochemical sensors by different modifiers is very interesting and there are different materials for modifying the electrodes. Fullerenes because of having unique electronic, structural and spectroscopic properties have obtained a lot of applications in different areas of science [15,16]. Fullerene C_{60} (C_{60}) is an electron acceptor and because of its unique dimensional and electronic structures has a rich electrochemistry [17]. The previous studies revealed that the partially reduced C_{60} films have favorable electrocatalytic properties and are sufficiently conductive for using in modifying the electrodes [18–22]. Metallic nanoparticles such as palladium nanoparticles (Pd NPs) due to having interesting properties such as electrocatalytic property, high surface area and conductivity are able to fasten the rate of electron transfer, therefore, they are frequently used in fabrication of electrochemical sensors [23,24]. Carbon nanotubes (CNTs) due to having some important electrochemical and mechanical properties such as high electron transfer rate, high surface area and stability and minimization of the surface fouling have obtained a lot of applications in fabrication of electrochemical sensors and biosensors [25]. Chitosan (CS) is a natural biopolymer with film-forming ability which can also play a role of stabilizer and dispersant [26]. The CS in

* Corresponding author.
E-mail addresses: ali.jalalvand1984@gmail.com, alireza.jalalvand@kums.ac.ir (A.R. Jalalvand).

https://doi.org/10.1016/j.talanta.2019.04.037
Received 19 January 2019; Received in revised form 9 April 2019; Accepted 14 April 2019
Available online 15 April 2019
0039-9140/

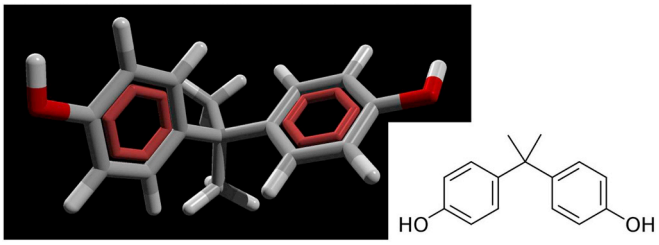

Fig. 1. Molecular structure of BPA.

combination with multiwalled carbon nanotubes (MWCNTs) can form a composite film with better electrochemical and mechanical properties than CS or MWCNTs [27].

In this work, we are going to fabricate a novel electrochemical biosensor based on step-by-step modification of a glassy carbon electrode (GCE) to monitor the DNA damage induced by BPA and to develop novel analytical methods for determination of BPA. Fabrication procedure applied to the GCE was included landing of methylene blue (MB) onto the surface of DNA/MWCNTs-CS/Pd NPs/C_{60}/GCE. MB is a derivative of anthraquinone which is able to intercalate into the double helix structure of DNA and can be used for the detection of damage on natural DNA. Fabrication procedure applied to the GCE to fabricate the biosensor has been summarized in Scheme 1.

2. Experimental

2.1. Chemicals and solutions

MB, CS, C_{60}, double-stranded calf thymus DNA, BPA (≥99%), dimethylformamide (DMF), KCl, acetic acid, CH_2Cl_2, phosphoric acid (H_3PO_4), sodium hydroxide, potassium ferrocyanide, potassium ferricyanide, palladium (II) chloride ($PdCl_2$), phosphate monobasic (NaH_2PO_4) and sodium phosphate dibasic (Na_2HPO_4) were purchased from Sigma. The MWCNTs were purchased from Ionic Liquid Technologies. The other chemicals used in this study were purchased from regular sources and used as received without any further purifications.

A phosphate buffer solution (PBS) with a concentration of 0.05 M and pH 7 was prepared. A solution of MWCNTs was prepared by dissolution of 10 mg of solid powder of MWCNTs in 1 mL DMF and ultrasonicated for 45 min. 10 mg CS was added to 1 mL acetic acid and ultrasonicated for 45 min. To prepare MWCNTs-CS, 0.5 mL CS was added to 0.5 mL MWCNTs and ultrasonicated for 20 min. The C_{60} solution was prepared by the addition of 1 mg C_{60} to 300 µL CH_2Cl_2. A redox probe solution, $[Fe(CN)_6]^{3-/4-}$, with a concentration of 0.005 M was prepared in the PBS (0.05 M, pH 7) and used as the electrolyte for electrochemical characterization of the modified electrodes. A MB solution with a concentration of 0.01 M was prepared in the PBS (0.05 M, pH 7). A solution of $PdCl_2$ with a concentration of 0.05 M was prepared in 0.025 M KCl. 100 mL stock solution of BPA with a concentration of 0.1 M was prepared by dissolution of 2.28 g of its solid powder in the PBS (0.05 M, pH 7) and the BPA working solutions were prepared by applying suitable dilutions to its stock solution. A DNA solution (1.0 mg mL^{-1}) was prepared by dissolving a suitable amount of DNA in 0.05 M NaCl solution.

2.2. Instruments and softwares

An Autolab PGSTAT302N-high performance controlled by the NOVA software was used to record the experimental data. pH adjustments were performed by an ELMEIRON pH meter (CP-411). Scanning electron microscopic (SEM) images were captured by a skilled operator with the help of a KYKY-EM3200 scanning electron microscope. In electrochemical experiments, a GCE, an Ag/AgCl and a Pt wire were acted as working, reference and counter electrode, respectively. The recorded electrochemical data was transferred to MATLAB (Version 7.14, MathWorks, Inc.) environment and smoothed when necessary. All the computations were performed on a DELL XPS laptop (L502X).

2.3. Fabrication of the biosensor

Prior to the modification of the GCE, it was well-polished by a silky pad which had been an immersed into the alumina slurry and then, the GCE was rinsed by DDW. Finally, the GCE was ultrasonicated in ethanol for 20 min and rinsed with DDW and left to be dried at room temperature. Modification of the GCE was started by drop-casting of 10 µL C_{60} onto its surface. To reduce the C_{60} film formed on the GCE surface, the electrode was immersed into a 1 M KOH and the potential was scanned in the range of 0.0 V to −1.5 V with a scan rate of 10 mV s^{-1} for 10 cycles. Then, electrodeposition of Pd NPs was performed by repetitive CV scanning from 0 to −1 for 8 cycles on the C_{60}/GCE immersed into 0.05 M $PdCl_2$ solution. For landing the third layer onto the surface of the electrode, 10 µL MWCNTs-CS was drop-casted onto the

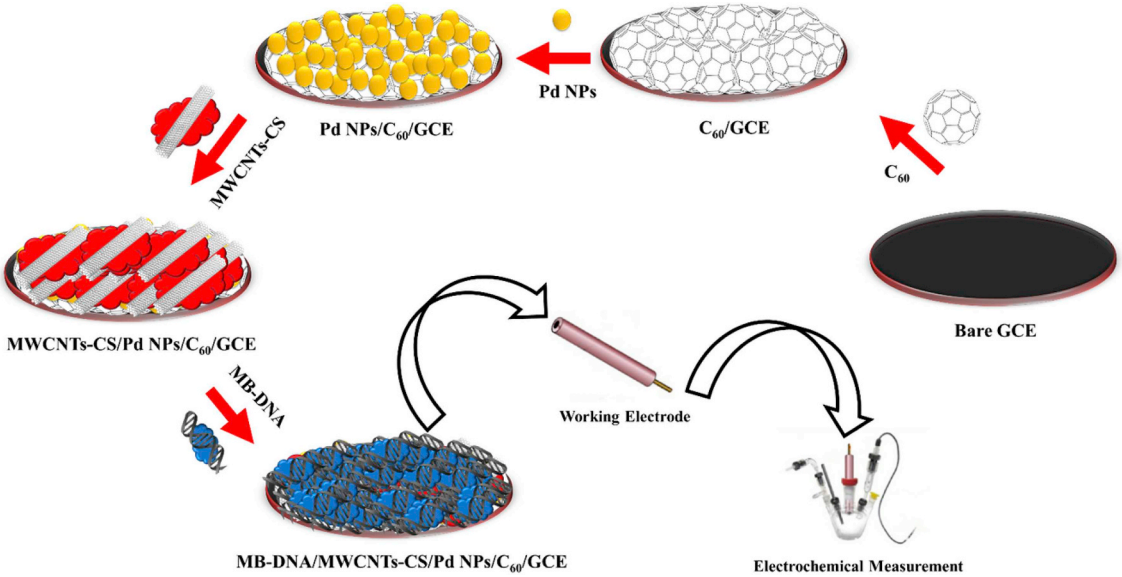

Scheme 1. Schematic representation of fabrication procedure applied to the GCE to fabricate MB-DNA/MWCNTs-CS/Pd NPs/C_{60}/GCE.

surface of Pd NPs/C_{60}/GCE and left to be dried at room temperature. Finally, 10 μL 1.0 mg mL^{-1} DNA solution was casted on the surface of the MWCNTs-CS/Pd NPs/C_{60}/GCE and left to be dried at room temperature and then, the sensor was washed with DDW and immersed into PBS (0.05 M, pH 7) for 5 min to remove any loosely adsorbed DNA. For loading of MB onto the surface of DNA/MWCNTs-CS/Pd NPs/C_{60}/GCE, the electrode was immersed into the 1 mM MB solution for 30 min and then, the electrode (MB-DNA/MWCNTs-CS/Pd NPs/C_{60}/GCE) was rinsed with PBS (0.05 M, pH 7) and kept in a refrigerator until analysis time.

3. Results and discussion

3.1. Characterization of the prepared biosensor

After fabrication of a biosensor, its structure must be characterized to prove the successfulness of the fabrication process. Characterization of the biosensor can be performed by electrochemical and microscopic techniques. Therefore, we have used cyclic voltammetry (CV), differential pulse voltammetry (DPV), electrochemical impedance spectroscopy (EIS) and SEM for characterizing the modifications applied to the GCE.

3.1.1. Characterization of the modifications by SEM

The surface of different modified electrodes was characterized by SEM and the results are shown in Fig. 2. The Fig. 2A showed that the C_{60} has formed a layer at the surface of GCE which was decorated by Pd NPs after electrosynthesizing the Pd NPs onto the surface of C_{60}/GCE. The SEM image captured from the surface of Pd NPs/C_{60}/GCE is shown in Fig. 2B. Characterization of MWCNTs-CS/Pd NPs/C_{60}/GCE by SEM showed an elegant image (Fig. 2C) in which tubes of MWCNTs have been integrated with CS to form a composite layer. By the presence of DNA at the surface of MWCNTs-CS/Pd NPs/C_{60}/GCE, the surface of the electrode was covered by a new layer in which some details of the previous layer can also be observed (Fig. 2D). On the whole, we think that the SEM was a successful method which helped us to observe the modifications used to fabricate the biosensor, but in next section more information about characterization of the modifications will be extracted by electrochemical techniques.

3.1.2. Electrochemical characterization of the modifications

Electrochemical methods are suitable methods which can help us to monitor and characterize the modifications applied to the GCE. Therefore, we have used CV, DPV and EIS for characterization the modifications. The CVs of different electrodes including GCE (curve *a*), C_{60}/GCE (curve *b*), Pd NPs/C_{60}/GCE (curve *c*), MWCNTs-CS/Pd NPs/C_{60}/GCE (curve *d*) and DNA/MWCNTs-CS/Pd NPs/C_{60}/GCE (curve *e*) in contacting with the redox probe solution, $[Fe(CN)_6]^{3-/4-}$, with a concentration of 0.005 M under scanning the potential with a rate of 50 mV s^{-1} are shown in Fig. 3A. Recording the response of the GCE showed a well-defined CV and after its modification with C_{60}, a noticeable improvement was observed in its response which can be clearly observed in curve *b*. The previous works reported on C_{60} showed that by partial reduction of C_{60} immobilized onto the electrode surface in aqueous solutions having potassium ions, conductive films are formed onto the electrode surface [28]. By the electrodeposition of Pd NPs onto the C_{60}/GCE surface, a new sensor with higher peaks' currents were fabricated which confirmed the role of NPs in improving the modification procedure. Drop-casting of MWCNTs-CS onto the surface of Pd NPs/C_{60}/GCE helped us to fabricate a new sensor whose performance was further improved. Finally, by the presence of DNA at the electrode surface, an electrostatic repulsion between DNA and the electrochemical probe carrying negative charge was occurred which caused a poorer response of the biosensor to the electrochemical probe [29].

The DPV is another electrochemical technique which has been used to characterize the modifications applied to the GCE to fabricate the biosensor. The DPV responses of different electrodes including GCE (curve *a*), C_{60}/GCE (curve *b*), Pd NPs/C_{60}/GCE (curve *c*), MWCNTs-CS/Pd NPs/C_{60}/GCE (curve *d*) and DNA/MWCNTs-CS/Pd NPs/C_{60}/GCE (curve *e*) in contacting with the redox probe solution, $[Fe(CN)_6]^{3-/4-}$, with a concentration of 0.005 M are shown in Fig. 3B (DPV conditions: step potential = 0.005 V, modulation amplitude = 0.025 V, modulation

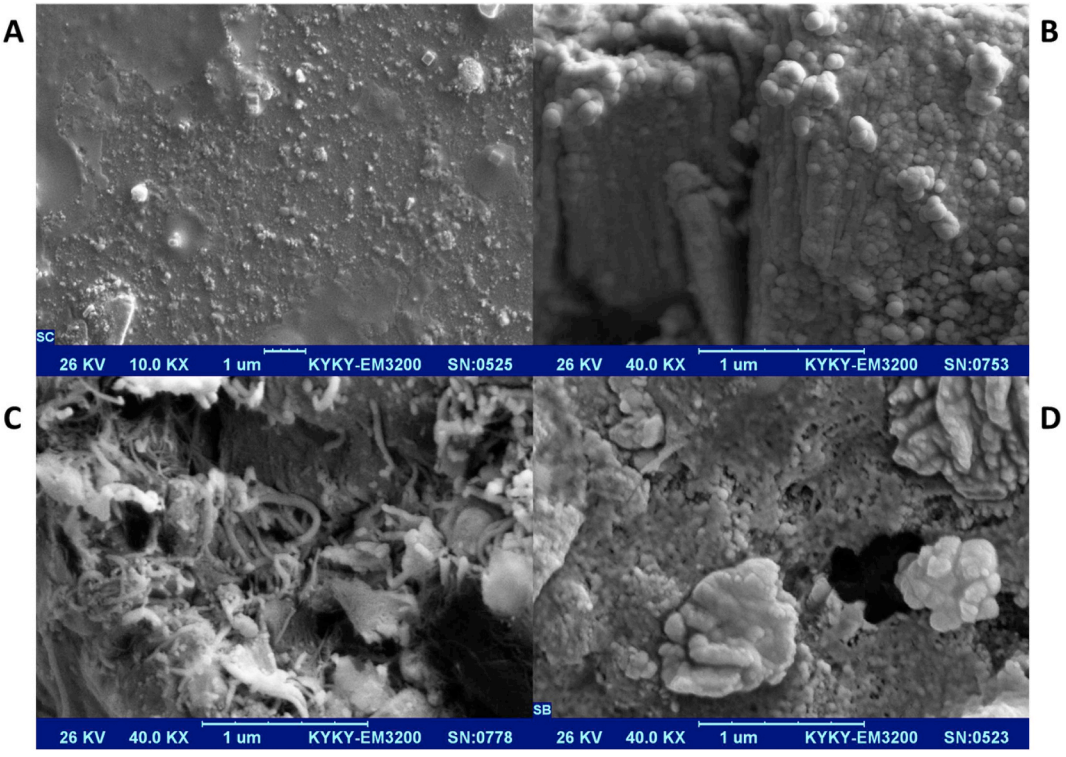

Fig. 2. SEM images captured from the surface of (A) C_{60}/GCE, (B) Pd NPs/C_{60}/GCE, (C) MWCNTs-CS/Pd NPs/C_{60}/GCE and (D) DNA/MWCNTs-CS/Pd NPs/C_{60}/GCE.

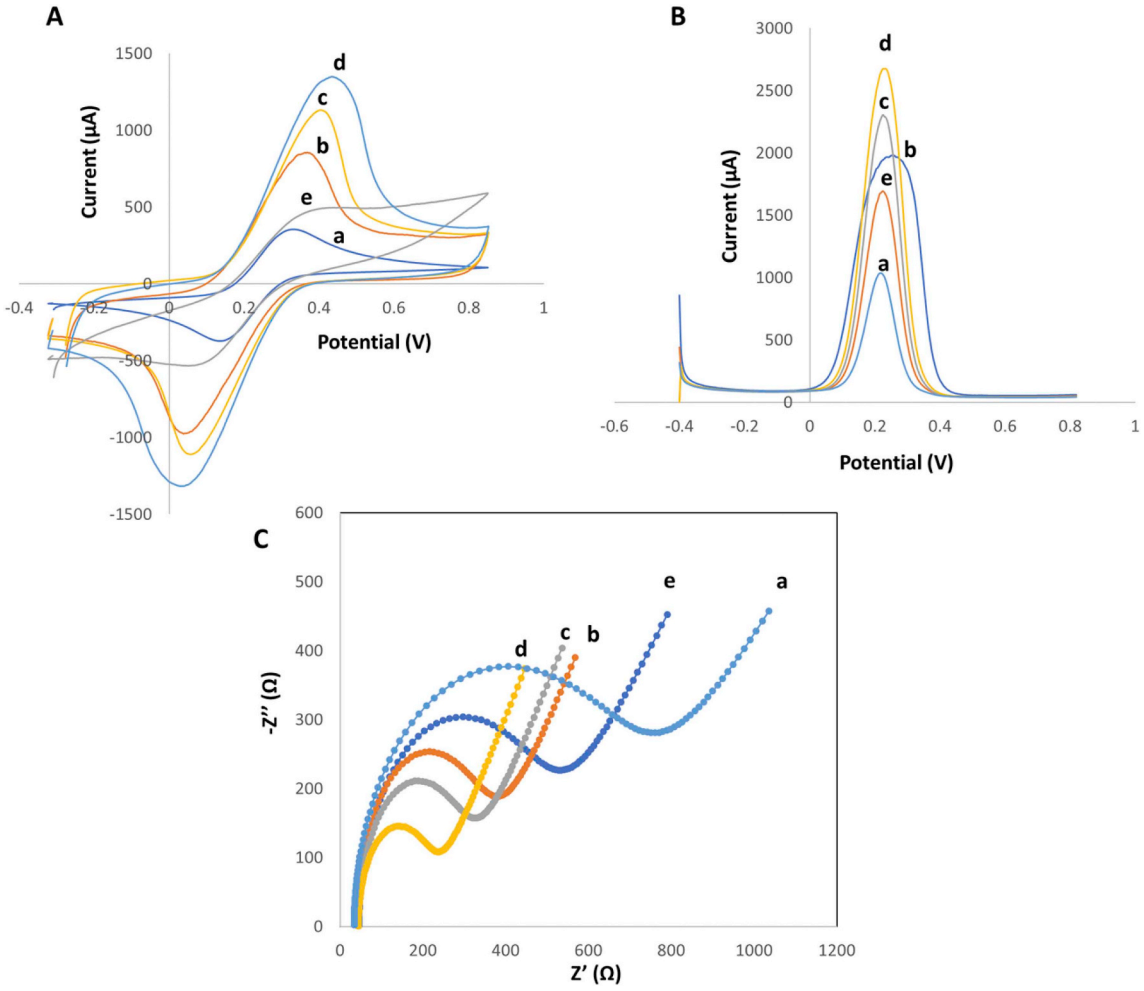

Fig. 3. (A) CVs, (B) DPVs (DPV conditions: step potential = 0.005 V, modulation amplitude = 0.025 V, modulation time = 0.05 s and interval time = 0.5 s) and (C) EISs of (a) GCE, (b) C_{60}/GCE, (c) Pd NPs/C_{60}/GCE, (d) MWCNTs-CS/Pd NPs/C_{60}/GCE and (e) DNA/MWCNTs-CS/Pd NPs/C_{60}/GCE in the redox probe solution, $[Fe(CN)_6]^{3-/4-}$, with a concentration of 0.005 M was prepared in the PBS (0.05 M, pH 7.0).

time = 0.05 s and interval time = 0.5 s). As can be seen, the results of DPV experiments are in a good agreement with the CV results which guaranteed the outcomes of CV experiments.

The EIS is a very important electrochemical technique by which the surface characteristics of the modified electrodes can be investigated. The output of an EIS experiment is a curve with a semicircle portion which its diameter reflects the charge transfer resistance (R_{ct}). After modification of the electrode surface, its R_{ct} is changed which causes a change in the diameter of the semicircle portion. Therefore, by investigation of the EIS curves, we will be able to investigate the surface properties of the modified electrodes. To achieve this goal, the EIS responses of different electrodes including GCE (curve *a*), C_{60}/GCE (curve *b*), Pd NPs/C_{60}/GCE (curve *c*), MWCNTs-CS/Pd NPs/C_{60}/GCE (curve *d*) and DNA/MWCNTs-CS/Pd NPs/C_{60}/GCE (curve *e*) in contacting with the redox probe solution, $[Fe(CN)_6]^{3-/4-}$, with a concentration of 0.005 M were recorded which are shown in Fig. 3C. The EIS curve of the GCE showed a semicircle with a diameter of 760 Ω and after modification of the GCE with C_{60}, the R_{ct} was decreased which confirmed the role of C_{60} in fastening the rate of charge transfer at the electrode surface. Further improvement in EIS response of the sensor was observed after its modification with Pd NPs. The presence of MWCNTs-CS onto the electrode surface caused a more facile electron transfer at the electrode surface. Finally, due to the presence of DNA and its repulsive interaction with the electrochemical probe carrying negative charge the R_{ct} was increased [29].

3.2. Loading of MB onto the surface of electrode

Loading of MB onto different electrodes including DNA/GCE, DNA/C_{60}/GCE, DNA/Pd NPs/C_{60}/GCE, DNA/CS/Pd NPs/C_{60}/GCE and DNA/MWCNTs-CS/Pd NPs/C_{60}/GCE was examined and the results are shown in Fig. 4. To achieve this goal, each electrode was immersed into 1 mM MB prepared in the PBS (0.05 M, pH 7) for 30 min, and then, rinsed with DDW. The DPVs of MB-DNA/GCE (curve *a*), MB-DNA/C_{60}/GCE (curve *b*), MB-DNA/Pd NPs/C_{60}/GCE (curve *c*), MB-DNA/CS/Pd NPs/C_{60}/GCE (curve *d*), MB-DNA/MWCNTs-CS/Pd NPs/C_{60}/GCE (curve *e*) and MB/MWCNTs-CS/Pd NPs/C_{60}/GCE (curve *f*) recorded in the PBS (0.05 M, pH 7) are shown in Fig. 4 (DPV conditions: step potential = 0.05 V, modulation amplitude = 0.035 V, modulation time = 0.05 s and interval time = 0.5 s). As can be seen, the highest current is related to MB-DNA/MWCNTs-CS/Pd NPs/C_{60}/GCE (curve *e*) which confirms that the DNA/MWCNTs-CS/Pd NPs/C_{60}/GCE has the highest capacity for MB loading among the tested electrodes. The current intensity of MB/MWCNTs-CS/Pd NPs/C_{60}/GCE was considerably lower than that of MB-DNA/MWCNTs-CS/Pd NPs/C_{60}/GCE which showed that the was MB interacted mainly with the DNA, and not the MWCNTs-CS/Pd NPs/C_{60}. This result can be justified by regarding that the DNA/MWCNTs-CS/Pd NPs/C_{60}/GCE has a large surface area, and thus, can absorb many DNA molecules.

Further investigation of the surface areas of the electrodes were evaluated by the Randles-Sevcik equation (298.15 K), using the redox currents of the redox probe (i_p) according the following equation:

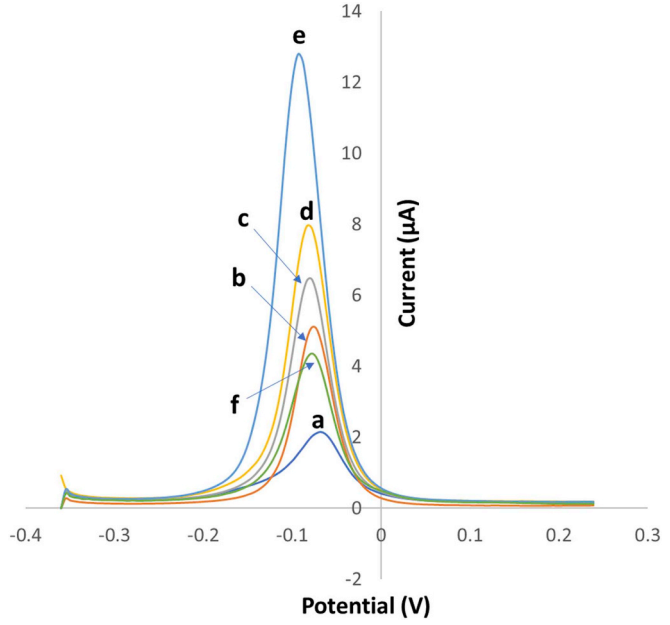

Fig. 4. DPVs of (a) MB-DNA/GCE, (b) MB-DNA/C_{60}/GCE, (c) MB-DNA/Pd NPs/C_{60}/GCE, (d) MB-DNA/CS/Pd NPs/C_{60}/GCE, (e) MB-DNA/MWCNTs-CS/Pd NPs/C_{60}/GCE and (f) MB/MWCNTs-CS/Pd NPs/C_{60}/GCE recorded in the PBS (0.05 M, pH 7). DPV conditions: step potential = 0.05 V, modulation amplitude = 0.035 V, modulation time = 0.05 s and interval time = 0.5 s.

$$i_p = (2.687 \times 10^5)\, n^{3/2}\, \upsilon^{1/2} D^{1/2} A C \quad (1)$$

where D, the diffusion coefficient of the ferricyanide, is $6.3 \times 10^{-6}\,cm^2\,s^{-1}$; i_p in amperes is the peak current; n and C are the transferring electron number ($n = 1$) and the concentration of the ferricyanide ($5 \times 10^{-6}\,mol\,cm^{-3}$), respectively; ν is the scan rate ($V\,s^{-1}$); and A is the surface area (cm^2). The surface areas of the bare GCE, C_{60}/GCE, Pd NPs/C_{60}/GCE and MWCNTs-CS/Pd NPs/C_{60}/GCE in contact with the electrochemical probe (0.005 M) were calculated to be 0.09, 0.16, 0.19 and 0.28 cm^2, respectively. As can be seen, the MWCNTs-CS/Pd NPs/C_{60}/GCE has the largest surface area which enables it for loading more DNA molecules. The surface concentration of DNA at DNA/MWCNTs-CS/Pd NPs/C_{60}/GCE was estimated according to the following equation:

$$I = n\,F\,\upsilon\,A\Gamma_c\,/4RT \quad (2)$$

where ν is the scan rate, A is related to the effective surface area of the electrode which is to be 0.28 cm^2, Γ_c is the surface concentration of DNA and the other symbols have their conventional meaning. The cathodic peak currents were plotted *vs.* ν and the slope of the plot was used to estimate the Γ_c of DNA which was to be $3.67 \times 10^{-4}\,mol\,cm^{-2}$.

3.3. Testing the loading/releasing of MB at the DNA/MWCNTs-CS/Pd NPs/C_{60}/GCE

For testing the reversibility of loading/releasing of MB at the surface of DNA/MWCNTs-CS/Pd NPs/C_{60}/GCE, the electrode which was loaded by MB was immersed into the PBS (0.05 M, pH 7) and its DPV response (DPV conditions: step potential = 0.05 V, modulation amplitude = 0.035 V, modulation time = 0.05 s and interval time = 0.5 s) was recorded which can be seen in Fig. 5 (curve *a*). Then, the electrode was immersed into the PBS (0.05 M, pH 7) for 3 h and its DPV response was recorded which is shown by curve *b*. During this period of time, some of the MB molecules which had been immobilized by non-specific binding, were released from the surface of DNA/MWCNTs-CS/Pd NPs/C_{60}/GCE. Therefore, the DPV response was decreased as is illustrated in curve *b*. Afterwards, the DNA/MWCNTs-CS/Pd NPs/C_{60}/GCE was re-immersed into the MB solution for reloading of MB onto the surface of electrode and then, its DPV response was recorded which is shown by curve *c*. As can be seen, the DPV response of the electrode is compatible with its first response. This result confirmed that the loading/releasing of MB at the surface of DNA/MWCNTs-CS/Pd NPs/C_{60}/GCE was readily reversible and the composite film on the electrode was quite stable and able to retain its original structure and binding capability.

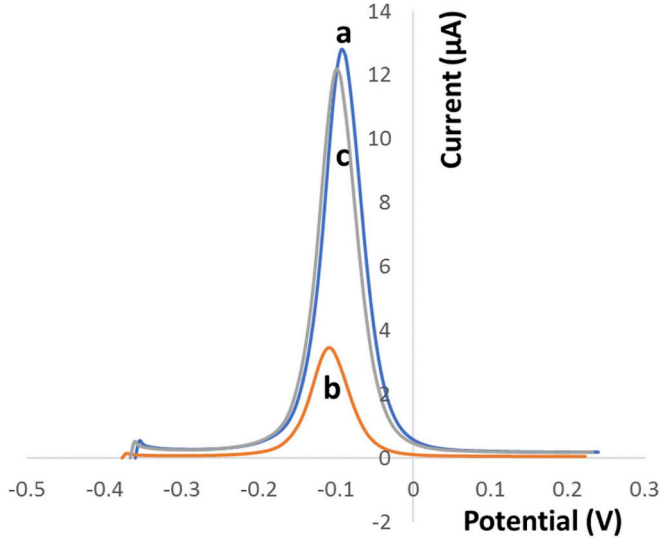

Fig. 5. DPVs of MB-DNA/MWCNTs-CS/Pd NPs/C_{60}/GCE (a) in the PBS (0.05 M, pH 7), (b) after immersing in the PBS (0.05 M, pH 7) for 3 h and (c) in the PBS (0.05 M, pH 7) after re-immersing in MB solution. DPV conditions: step potential = 0.05 V, modulation amplitude = 0.035 V, modulation time = 0.05 s and interval time = 0.5 s.

3.4. Detection of DNA damage by DPV

In order to monitor the DNA damage induced by BPA, the DPV responses of MB-DNA/MWCNTs-CS/Pd NPs/C_{60}/GCE under incubation with different concentrations of BPA were recorded which can be seen in Fig. 6A (DPV conditions: step potential = 0.05 V, modulation amplitude = 0.015 V, modulation time = 0.05 s and interval time = 0.5 s). To record these DPV responses, the MB-DNA/MWCNTs-CS/Pd NPs/C_{60}/GCE was incubated in BPA solutions with different concentrations ranging in 1–50 μM BPA for 10 min and then, the biosensor was immersed into the PBS (0.05 M, pH 7) and its DPV response was recorded. As can be seen, the peak currents are decreased with increasing concentration of BPA. This indicated that the DNA films damaged by BPA cannot reload as much MB as with the undamaged DNA films, and thus, this observation suggested that the interaction between BPA and DNA was irreversible. In order to develop an indirect method for the determination of BPA the current differences were regressed on BPA concentrations to build a calibration curve which can be seen in Fig. 6B. The limit of detection (LOD) of this method was calculated to be 0.5 μM according to IUPAC recommendations ($3S_b/b$, where S_b is the standard deviation (n = 5) of the blanks, and b is the slope value of the respective calibration graph) and the limit of quantitation (LOQ, $10S_b/b$) was calculated to be 1.41 μM. Therefore, according to the monitoring of DNA damage induced by BPA, an indirect DPV method was developed for determination of BPA.

3.5. Detection of DNA damage by EIS

In this section, our study was expanded to monitor the DNA damage induced by BPA with the help of EIS method and to achieve this goal, the MB-DNA/MWCNTs-CS/Pd NPs/C_{60}/GCE was incubated in BPA

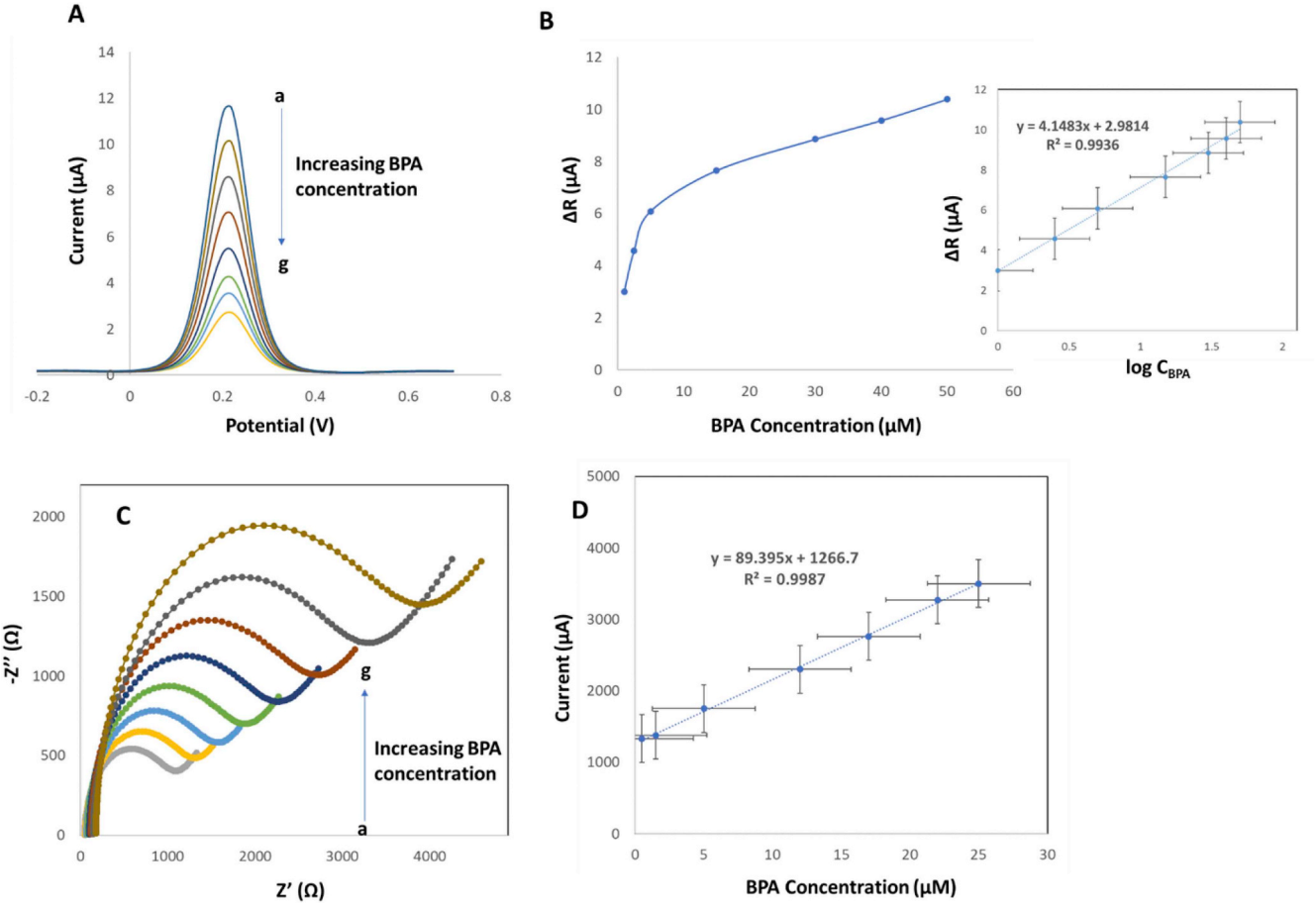

Fig. 6. (A) DPVs of MB-DNA/MWCNTs-CS/Pd NPs/C_{60}/GCE in the PBS (0.05 M, pH 7) after incubating in BPA solution with different concentrations ranging in 1–50 μM ((a) 1 μM, (b) 2.5 μM, (c) 5 μM, (d) 15 μM, (e) 30 μM, (f) 40 μM and (g) 50 μM), DPV conditions: step potential = 0.05 V, modulation amplitude = 0.015 V, modulation time = 0.05 s and interval time = 0.5 s. (B) the calibration curve obtained by regressing DPV differences on BPA concentrations, (C) EISs of MB-DNA/MWCNTs-CS/Pd NPs/C_{60}/GCE after incubating in BPA solution with different concentrations ranging in 0.5–25 μM ((a) 0.5 μM, (b) 1.5 μM, (c) 5 μM, (d) 12 μM, (e) 17 μM, (f) 22 μM and (g) 25 μM) and (D) the calibration curve obtained by regressing R_{ct} values on BPA concentrations.

Table 1
Results of other published methods for the determination of BPA in comparison with the method from this work.

Senor	Linear range	LOD	Ref.
Laccase-thionine-carbon black	0.05–1 μM	0.2 μM	[31]
Tyr/thionine/CP	0.15–45 μM	0.15 μM	[32]
CS–Fe_3O_4/GCE	50 nM-3 × 10^{-5} M	8 nM	[33]
CS/MNPs-rGO/GCE	6 × 10^{-8} M − 11 μM	16.7 nM	[34]
Graphene nanofibers–AuNPs/GCE	8 × 10^{-8} M − 25 μM	35 nM	[35]
Bi_2WO_6–CPE	5 × 10^{-8} M-13 × 10^{-7} M	15 nM	[36]
MB-DNA/MWCNTs-CS/Pd NPs/C_{60}/GCE	1–50 μM and 0.5–25 μM	0.5 μM and 0.35 μM	This work

solutions having different concentrations ranging in 0.5–25 μM BPA for 10 min and then, the biosensor was rinsed with PBS (0.05 M, pH 7) and immersed into the electrochemical probe and its EIS response was recorded. The results are shown in Fig. 6C and as can be seen, the semicircle portion of the EIS curves are increasing with increasing concentration of BPA. This possibly occurred because the insertion of BPA molecules into the DNA reduces its charge transport. The insertion of the BPA molecules may result in a more negative charge environment on the DNA surface, which hinders accessibility of the $[Fe(CN)_6]^{3-/4-}$ anion. This may form a steric barrier at the base of the DNA structure, which decreases the charge transport contribution of the DNA [30]. In order to develop an indirect method for the determination of BPA, the EIS differences were regressed on BPA concentrations to build a calibration curve which can be seen in Fig. 6D. The LOD of this method was calculated to be 0.35 μM and the LOQ was calculated to be 1.03 μM. Therefore, according to the EIS monitoring of DNA damage induced by BPA, an indirect EIS method was developed for determination of BPA.

3.6. Repeatability, reproducibility and stability of the biosensor

In order to investigate the stability of the developed biosensor, its DPV response was recorded during two weeks and our records confirmed that the biosensor was able to retain 97.3% of its original response which confirmed that the biosensor response was stable. The reproducibility of the biosensor was also investigated by constructing five biosensors and recording their DPV response for six times. The results showed a relative standard deviation (RSD) of 4.05% which conformed that the biosensor response was reproducible. The repeatability of the biosensor was investigated by recording its DPV response to 10 μM BPA for six times during a day and our records showed a RSD of 3.66% which conformed a repeatable response for the developed biosensor.

3.7. Comparison with the other works published in the literature

In this section, we have compared the performance of the developed biosensor in this study for determination of BPA and detection of DNA damage with the previous works and the results have been arranged in

Table 2
Comparing this work with the previous works focused on detection of DNA damage.

Sensor	Method	DNA attachment method	Long term stability	Ref.
CS/ds-DNA/Ag-PGL/GCE	LSV	Adsorption	15 days	[37]
DNA–XOD/GCE	SWV	Adsorption	7 days	[38]
DNA–XOD/GCE	SWV	Adsorption	–	[39]
dsDNA/GCE	SWV	Adsorption	–	[40]
(MWCNTs/PDDA/ds-DNA)$_2$/PGE	DPV	Layer by layer	–	[41]
(PDDA/dsDNA)3/GCE	CV	Layer by layer	30 days	[42]
DNA/GCE	SWV	Adsorption	–	[43]
DNA/AuNPs/SPGE	EIS	Covalent attachment	21 days	[44]
MB-DNA/MWCNTs-CS/Pd NPs/C_{60}/GCE	EIS and DPV	Layer by layer	14 Days	This work

Tables 1 and 2. However, the main aim of this work was focused on developing a method for detection of DNA damage induced by BPA, but the developed biosensor had an acceptable performance for determination of BPA as well. Therefore, the biosensor had an acceptable performance in detention of DNA damage and determination of BPA.

4. Conclusions

In this work, a novel electrochemical biosensor was fabricated for impedimetric and voltammetric detection of DNA damage induced by BPA based on step-by-step modification of a GCE with MB-DNA/MWCNTs-CS/Pd NPs/C_{60} as a composite film. In this modified electrode, the MB was acted as an electroactive probe which enabled us to monitor the DNA damage induced by BPA. The results confirmed that the loading-releasing of MB was readily reversible. According to the results obtained for the detection of DNA damage, two voltammetric and impedimetric methods were developed for determination of BPA. The efficiency of this method is derived from the inherent rapidity of the electrochemical transducers, and the high sensitivity is due to the high surface-to-volume ratio and good in-plane conductivity caused by the presence of MWCNTs-CS, Pd NPs and C_{60} which made effective signal amplification. Therefore, this biosensor combines the advantages of suitable modification and the power of electrochemical detection techniques to provide an option for detection of DNA damage.

Acknowledgements

Hereby, the authors appreciate the financial supports of this project by the research council of Kermanshah University of medical Science.

Appendix A. Supplementary data

Supplementary data to this article can be found online at https://doi.org/10.1016/j.talanta.2019.04.037.

References

[1] X. Yu, Y. Chen, L. Chang, L. Zhou, F. Tang, X. Wu, β-cyclodextrin non-covalently modified ionic liquid-based carbon paste electrode as a novel voltammetric sensor for specific detection of bisphenol A, Sensor. Actuator. B Chem. 186 (2013) 648–656.
[2] A. Ballesteros-Gomez, S. Rubio, D. Perez-Bendito, Analytical methods for the determination of bisphenol A in food, J. Chromatogr. A 1216 (2009) 449–469.
[3] K.V. Ragavan, N.K. Rastogi, M.S. Thakur, Sensors and biosensors for analysis of bisphenol-A, Trends Anal. Chem. 52 (2013) 248–260.
[4] D.H. Atha, N. Ammanamanchi, M. Obadina, V. Reipa, Quantitative measurement of electrochemically induced DNA damage using capillary electrophoresis, J. Electrochem. Soc. 160 (2013) G3139–G3143.
[5] D. Anderson, J. Laubenthal, Analysis of DNA damage via single-cell electrophoresis, Methods Mol. Biol. 1054 (2013) 209–218.
[6] R.M. Vlad, M.C. Kolios, G.J. Gregory, Ultrasound imaging of apoptosis: spectroscopic detection of DNA-damage effects at high and low frequencies, DNA damage detection in situ, ex vivo, and in vivo: methods and protocols, Methods Mol. Biol. 682 (2011) 165–187.
[7] M. Frontini, M. Vijayakumar, A. Garvin, N. Clarke, A ChIP chip approach reveals a novel role for transcription factor IRF1 in the DNA damage response, Nucleic Acids Res. 37 (2009) 1073–1085.
[8] Y.N. Ni, P.P. Wang, H.Y. Song, X.Y. Lin, S. Kokot, Electrochemical detection of benzo(a) pyrene and related DNA damage using DNA/hemin/nafion-graphene biosensor, Anal. Chim. Acta 821 (2014) 34–40.
[9] T.L. Liao, Y.F. Wang, X.B. Zhou, Y. Zhang, X.H. Liu, J. Du, X.J. Li, X.Q. Lu, Detection of DNA damage induced by styrene oxide in dsDNA layer-by-layer films using adriamycin as electroactive probe, Colloids Surf., B 76 (2010) 334–339.
[10] S. Carlos, B. Oliveira, A.M. Oliveira-Brett, In situ DNA oxidative damage by electrochemically generated hydroxyl free radicals on a boron-doped diamond electrode, Langmuir 28 (2012) 4896–4901.
[11] L.P. Lu, L.H. Xu, T.F. Kang, S.Y. Cheng, Investigation of DNA damage treated with perfluorooctane sulfonate (PFOS) on ZrO2/DDAB active nano-order film, Biosens. Bioelectron. 35 (2012) 180–185.
[12] W. Dekant, W. Völkel, Human exposure to bisphenol A by biomonitoring: methods, results and assessment of environmental exposures, Toxicol. Appl. Pharmacol. 228 (2008) 114–134.
[13] M.B. Gholivand, A.R. Jalalvand, H.C. Goicoechea, G. Paimard, T. Skov, Surface exploration of a roomtemperature ionic liquid-chitin composite film decorated with electrochemically deposited PdFeNi trimetallic alloy nanoparticles by pattern recognition: an elegant approach to developing a novel biotin biosensor, Talanta 131 (2015) 249–258.
[14] M.B. Gholivand, A.R. Jalalvand, H.C. Goicoechea, T. Skov, Chemometrics-assisted simultaneous voltammetric determination of ascorbic acid, uric acid, dopamine and nitrite: application of non-bilinear voltammetric data for exploiting first-order advantage, Talanta 119 (2014) 553–563.
[15] M.M. Zangeneh, H. Norouzi, M. Mahmoudi, H.C. Goicoechea, A.R. Jalalvand, Fabrication of a novel impedimetric biosensor for label free detection of DNA damage induced by doxorubicin, Int. J. Biol. Macromol. 124 (2019) 963–971.
[16] E. Nakamura, H. Isobe, Functionalized fullerenes in water. the first 10 years of their chemistry, biology, and nanoscience, Acc. Chem. Res. 36 (2003) 807.
[17] C.A. Martin, D. Ding, J.K. Sørensen, T. Bjørnholm, J.M. van Ruitenbeek, H.S.J. van der Zant, Fullerene-based anchoring groups for molecular electronics, J. Am. Chem. Soc. 130 (2008) 13198–13199.
[18] B.C. Thompson, J.M.J. Frechet, Polymer-fullerene composite solar cells, Angew Chem. Int. Ed. Engl. 47 (2008) 58–77.
[19] E. Grodzka, P. Pieta, P. Dluzewski, W. Kutner, K. Winkler, Formation and electrochemical properties of composites of the C_{60}–Pd polymer and multi-wall carbon nanotubes, Electrochim. Acta 54 (2009) 5621–5628.
[20] M. Csiszar, A. Szucs, M. Tolgyesi, A. Mechler, J.B. Nagy, M.J. Novak, Electrochemical reactions of cytochrome *c* on electrodes modified by fullerene films, J. Electroanal. Chem. 497 (2001) 69–74.
[21] R.N. Goyal, V.K. Gupta, N. Bachheti, R.A. Sharma, Electrochemical sensor for the determination of dopamine in presence of high concentration of ascorbic acid using a fullerene-C_{60} coated gold electrode, Electroanalysis 20 (2008) 757–764.
[22] N. Sun, L. Guan, Z. Shi, Z. Zhu, N. Li, M. Li, Z. Gu, Electrochemistry of fullerene peapod modified electrodes, Electrochem. Commun. 7 (2005) 1148–1152.
[23] O. Akyıldırım, F. Kardaş, M. Beytur, H. Yuksek, N. Atar, M.L. Yola, Palladium nanoparticles functionalized graphene quantum dots with molecularly imprinted polymer for electrochemical analysis of citrinin, J. Mol. Liq. 243 (2017) 677–681.
[24] Z. Liu, Q. Xue, Y. Guo, Sensitive electrochemical detection of rutin and isoquercitrin based on SH-β-cyclodextrin functionalized graphene-palladium nanoparticles, Biosens. Bioelectron. 89 (2017) 444–452.
[25] G.A. Rivas, M.D. Rubianes, M.C. Rodrıguez, N.F. Ferreyra, G.L. Luque, M.L. Pedano, S.A. Miscoria, C. Parrado, Carbon nanotubes for electrochemical biosensing, Talanta 74 (2007) 291–307.
[26] B. Krajewska, Application of chitin-and chitosan-based materials for enzyme immobilizations: a review, Enzym. Microb. Technol. 35 (2004) 126–139.
[27] Y. Li, Y. Li, Y. Yang, Direct electrochemistry and electrocatalysis of myoglobin-based nanocomposite membrane electrode, Bioelectrochemistry 82 (2011) 112-11.
[28] S.Z. Mousavisani, J.B. Raoof, R. Ojani, Z. Bagheryan, An impedimetric biosensor for DNA damage detection and study of the protective effect of deferoxamine against DNA damage, Bioelectrochemistry 122 (2018) 142–148.
[29] R.N. Goyal, V.K. Gupta, N. Bachheti, Fullerene-C_{60}-modified electrode as a sensitive voltammetric sensor for detection of nandrolone—an anabolic steroid used in doping, Anal. Chim. Acta 597 (2007) 82–89.
[30] L.P. Lu, L.H. Xu, T.F. Kang, S.Y. Cheng, Investigation of DNA damage treated with perfluorooctane sulfonate (PFOS) on ZrO2/DDAB active nano-order film, Biosens. Bioelectron. 35 (2012) 180–185.
[31] M. Portaccio, D. Di Tuoro, F. Arduini, D. Moscone, M. Cammarota, D.G. Mita, M. Lepore, Laccase biosensor based on screen-printed electrode modified with

thionine–carbon black nanocomposite, for bisphenol A detection, Electrochim. Acta 109 (2013) 340.
[32] M. Portaccio, D. Di Tuoro, F. Arduini, M. Lepore, D.G. Mita, N. Diano, L. Mita, D. Moscone, A thionine-modified carbon paste amperometric biosensor for catechol and bisphenol A determination, Biosens. Bioelectron. 25 (2010) 2003.
[33] C.M. Yu, L. Gou, X.H. Zhou, N. Bao, H.Y. Gu, Chitosan–Fe3O4 nanocomposite based electrochemical sensors for the determination of bisphenol A, Electrochim. Acta 56 (2011) 9056–9063.
[34] Y.X. Zhang, Y.X. Cheng, Y.Y. Zhou, B.Y. Li, W. Gu, Y.Z. Xian, Electrochemical sensor for bisphenol A based on magnetic nanoparticles decorated reduced graphene oxide, Talanta 107 (2013) 211–218.
[35] G.F. Pereira, L.S. Andrade, R.C. Rocha, N. Bochi, S.R. Biaggir, Electrochemical determination of bisphenol A using a boron-doped diamond electrode, Electrochim. Acta 82 (2012) 3–8.
[36] L. Peng, S. Dong, H. Xie, G. Gu, Z. He, J. Lu, T. Huang, Sensitive simultaneous determination of diethylstilbestrol and bisphenol A based on Bi2WO6 nanoplates modified carbon paste electrode, J. Electroanal. Chem. 726 (2014) 15-2.
[37] X. Wang, C. Jiao, Z. Yu, Electrochemical biosensor for assessment of the total antioxidant capacity of orange juice beverage based on the immobilizing DNA on a poly lglutamic acid doped silver hybridized membrane, Sensor. Actuator. B Chem. 192 (2014) 628–633.
[38] H. Xiong, Y. Chen, X. Zhang, H. Gu, S. Wang, An electrochemical biosensor for the rapid detection of DNA damage induced by xanthine oxidase-catalyzed Fenton reaction, Sensor. Actuator. B Chem. 181 (2013) 85–91.
[39] Y. Chen, H. Xiong, X. Zhang, S. Wang, Electrochemical detection of in situ DNA damage induced by enzyme-catalyzed Fenton reaction. Part I: in phosphate buffer solution, Microchim. Acta 178 (2012) 37–43.
[40] A. Hájková, J. Barek, V. Vyskočil, Electrochemical DNA biosensor for detection of DNA damage induced by hydroxyl radicals, Bioelectrochemistry 116 (2017) 1–9.
[41] A.A. Ensafi, M. Amini, B. Rezaei, Detection of DNA damage induced by chromium/glutathione/H2O2 system at MWCNTs–poly (diallyldimethylammonium chloride) modified pencil graphite electrode using methylene blue as an electroactive probe, Sensor. Actuator. B Chem. 177 (2013) 862–870.
[42] W. Zhang, T. Yang, W. Li, G. Li, K. Jiao, Rapid and sensitive electrochemical sensing of DNA damage induced by V2O5 nanobelts/HCl/H_2O_2 system in natural dsDNA layer-by-layer films, Biosens. Bioelectron. 25 (2010) 2370–2374.
[43] Y. Wang, H. Xiong, X. Zhang, S. Wang, Electrochemical biosensors for the detection of oxidative DNA damage induced by Fenton reagents in ionic liquid, Sensor. Actuator. B Chem. 161 (2012) 274–278.
[44] S.Z. Mousavisani, J.B. Raoof, R. Ojani, Z. Bagheryan, An impedimetric biosensor for DNA damage detection and study of the protective effect of deferoxamine against DNA damage, Bioelectrochemistry 122 (2018) 142–148.